

# Pauli Hardness Study of the Methane, Ammonia, Water and Hydrogen Fluoride Molecules

Edyta Małolepsza and Lucjan Piela

Department of Chemistry, University of Warsaw, Pasteura 1, 02-093 Warsaw, Poland

Received: February 19, 2003; In Final Form: May 6, 2003

A hardness of molecular surface (investigated by using the helium atom probe) is proposed as its descriptor. As an example, a homological series of the first-row hydrides has been studied. The molecular surface (“molecular shape”) is defined as an isosurface of the valence repulsion energy that is related to the Pauli exclusion principle. Interestingly, the amplitude of the surface–heavy atom distance is almost the same for all of the molecules, except the methane molecule, for which it is larger by about 33%. The Pauli hardness of a point on the isosurface is defined as the first derivative of the valence repulsion energy in the direction normal to the isosurface. Higher-order derivatives correspond to the nonlinear effects (hyperhardnesses). It turned out that the molecular surfaces of these molecules are convex and the Pauli hardness of a molecule varies within about 20% as a function of position on the molecular surface. The quantity also changes by about 30% among the molecules of the series. The molecule with the greatest Pauli hardness in the series is hydrogen fluoride, and the maximum Pauli hardness increases almost linearly with the atomic number of the heavy atom in the homological series studied. The minimum Pauli hardness behaves in a different way: it is the largest for the hydrogen fluoride and then decreases for the water and ammonia, while the methane molecule represents a remarkable exception showing considerable increase of this quantity. As a result, the methane molecule exhibits the smallest, while the ammonia molecule the largest, hardness anisotropy among the first-row hydrides.

## I. Introduction

Cohesive properties of complexes, liquids, and solids result from intermolecular interactions.<sup>1,2</sup> At large intermolecular distances, a dominant contribution to the interaction energy is usually the electrostatic one, defined as the Coulombic interaction of the unperturbed (“frozen”) charge distributions of the individual molecules. At intermediate distances, the dispersion and induction contributions increase to such an extent that they come additionally into play (as well as some higher-order terms of smaller importance).<sup>3</sup> The induction and dispersion forces are always attractive, while the electrostatic forces may be either repulsive or attractive depending usually on the mutual orientation of the molecules in space. Because the dispersion and induction contributions are much less orientation-dependent, the electrostatics often decides about mutual orientation of the interacting molecules, thus contributing to an additional attraction.<sup>2,4</sup>

The notions of all these contributions come from the polarization approximation in the Rayleigh–Schrödinger perturbational theory of intermolecular forces,<sup>1</sup> in which the zero-order wave function,  $\varphi^{(0)}$ , is assumed as a *product* of the normalized solutions to the Schrödinger equation for the individual molecules,  $\varphi^{(0)} = \varphi_A \varphi_B$ .

For closed-shell subsystems at short intermolecular distances, all of these effects are overcome by the valence repulsion, which represents the topic of the present paper. This quantity increases very rapidly<sup>5</sup> when the two subsystems approach. The valence repulsion appears as a result of the Pauli exclusion principle or the (necessary) antisymmetry of the total wave function with respect to exchange of labels between any two electrons of the system.

The valence repulsion is absent in the polarization approximation because the Pauli principle is not fulfilled by the

product-like  $\varphi^{(0)}$ . In the so-called symmetry-adapted perturbation theory (SAPT<sup>6</sup>), the zero-order wave function is taken as the *antisymmetrized product*,  $\psi^{(0)} = N \hat{\mathcal{A}} \varphi^{(0)}$  (called also the Heitler–London function), where  $N$  is a normalization constant and  $\hat{\mathcal{A}}$  stands for the idempotent ( $\hat{\mathcal{A}}^2 = \hat{\mathcal{A}}$ ) antisymmetrizer.

The first-order SAPT energy correction,

$$E^{(1)} = \frac{\langle \varphi^{(0)} | \hat{\mathcal{A}} \hat{V} \varphi^{(0)} \rangle}{\langle \varphi^{(0)} | \hat{\mathcal{A}} \varphi^{(0)} \rangle} \quad (1)$$

is called also the *Heitler–London interaction energy*,  $E_{\text{HL}}$ ,

$$E_{\text{HL}} = \langle \psi^{(0)} | \hat{H} \psi^{(0)} \rangle - (E_A + E_B) \quad (2)$$

because as it may be easily shown for the *exact* wave functions  $\varphi_A$  and  $\varphi_B$

$$E^{(1)} = E_{\text{HL}} \quad (3)$$

where  $\hat{H}$  is the electronic Hamiltonian,  $\hat{V}$  is the intermolecular interaction operator composed of all Coulombic interactions of the particles (electrons and nuclei) of monomer A with those of monomer B, and  $E_A$  and  $E_B$  represent the exact monomer energies.

The  $E_{\text{HL}}$  consists of the electrostatic and valence-repulsion ( $E_{\text{rep}}$ ) interactions; therefore,

$$E_{\text{rep}} = E_{\text{HL}} - E_{\text{elst}} \quad (4)$$

with the electrostatic energy,  $E_{\text{elst}}$  (identical to that appearing within the polarization approximation), defined as

$$E_{\text{elst}} = \langle \varphi^{(0)} | \hat{V} \varphi^{(0)} \rangle \quad (5)$$

The electrostatic energy may be split into a part that is representable by the multipole–multipole interactions<sup>1</sup> (the permanent multipole moments of the isolated subsystems),  $E_{\text{multipol}}$ , and a remainder,  $E_{\text{pen}}$ , the penetration energy that is a correction to the Coulombic interaction coming from interpenetration of the interacting charge distributions (it decays extremely fast with increasing distance)

$$E_{\text{elst}} = E_{\text{multipol}} + E_{\text{pen}} \quad (6)$$

Within the Born–Oppenheimer approximation the concept of a *molecular shape* (or a molecular surface) is often used. One may define a molecular shape in different ways (a quantum mechanical approach to this problem is presented in ref 7). The molecular surface concept, albeit to some extent arbitrary, is of crucial importance in understanding chemistry and biology (molecular recognition).

In the present paper, we use a definition of the molecular surface that highlights the valence repulsion of two subsystems: a molecule under study and a simple *structureless spherically symmetric atomic probe*—the ground-state helium atom. In that we follow Amovilli and McWeeny<sup>7</sup> and Stone and Tong,<sup>8</sup> in such a case (zero electric multipole moments of the probe), the valence repulsion interaction energy is reduced to the formula

$$E_{\text{rep}} = E_{\text{HL}} - E_{\text{pen}} \quad (7)$$

## II. The Pauli Molecular Hardness and Softness

Having defined the molecular shape as the valence repulsion isosurface, one may be interested in how easily the probe penetrates the isosurface, that is, in the hardness of a particular spot on the isosurface. This problem attracted attention in the literature for a long time, first for atoms and mononuclear ions<sup>9</sup> and then for molecules (nitrogen, chlorine, acetylene, and hydrogen sulfide<sup>8</sup>), but the emphasis has been put on approximate expressions for the valence repulsion energy rather than on the hardness distribution on the molecular surface.

The Pauli hardness,  $h^{(1)}$ , is defined as the first derivative of the valence repulsion energy computed at a given point of the valence repulsion +5 kcal mol<sup>-1</sup> isosurface (similarly as in ref 7) in the direction  $\nabla E_{\text{rep}}$ , that is, normal to this isosurface:

$$h^{(1)} = - \left( \frac{\partial}{\partial r} E_{\text{rep}} \right) \Big|_{r=0} \quad (8)$$

where  $r = 0$  corresponds to the point of the isosurface.

One may also define the higher hardnesses (*hyperhardnesses*)

$$h^{(n)} = (-1)^n \left( \frac{\partial^n}{\partial r^n} E_{\text{rep}} \right) \Big|_{r=0}, \quad n = 2, 3, \dots$$

calculated as higher-order derivatives in the direction perpendicular to the isosurface. For the sake of convenience, one may define additionally, as opposite to the Pauli hardness and hyperhardnesses ( $h^{(n)}$ ), the Pauli softness and hypersoftnesses,  $s(n) = 1/h^{(n)}$  for  $n = 1, 2, \dots$

**Numerical Details.** For  $\tilde{\varphi}_A$  and  $\tilde{\varphi}_B$  being some approximations to the exact solutions  $\varphi_A$  and  $\varphi_B$ , the  $E_{\text{HL}}$  computed from eq 2 and  $E^{(1)}$  of eq 1 are no longer equal one another and the difference,  $\Delta_{\text{LM}}$ , can be written in the following form:<sup>10,11</sup>

$$\Delta_{\text{LM}} = E_{\text{HL}} - E^{(1)} = \frac{\langle \tilde{\varphi}^{(0)} | \hat{\mathcal{L}}(\hat{H}_A + \hat{H}_B) | \tilde{\varphi}^{(0)} \rangle}{\langle \tilde{\varphi}^{(0)} | \hat{\mathcal{L}} | \tilde{\varphi}^{(0)} \rangle} - \langle \tilde{\varphi}^{(0)} | \hat{H}_A + \hat{H}_B | \tilde{\varphi}^{(0)} \rangle \quad (9)$$

where  $\tilde{\varphi}^{(0)} = \tilde{\varphi}_A \tilde{\varphi}_B$ .

The self-consistent field (SCF) linear combination of atomic orbitals (LCAO) molecular orbital (MO) approximations to the wave functions of the isolated interacting species ( $\tilde{\varphi}_A$  and  $\tilde{\varphi}_B$ ) have been used, and therefore, according to eq 9, the valence repulsion energy has been computed from eq 7 with

$$E_{\text{HL}} = E^{(1)} + \Delta_{\text{LM}} \quad (10)$$

In the case of the Hartree–Fock solutions, one may write  $\hat{H}_X = \hat{F}_X + \hat{W}_X$ , where  $\hat{F}_X$  is the sum of the Fock operators for the monomer X and  $\hat{W}_X = \hat{H}_X - \hat{F}_X$  is the so-called fluctuation potential. In such a case,  $\Delta_{\text{LM}}$  can be split into  $\Delta_{\text{LM}} = \Delta_{\text{L}} + \Delta_{\text{M}}$ , where  $\Delta_{\text{L}}$  is the so-called Landshoff's delta<sup>10</sup> and  $\Delta_{\text{M}}$  stands for the so-called Murrell's delta:<sup>11</sup>

$$\Delta_{\text{L}} = \sum_{X=A,B} \frac{\langle \tilde{\varphi}^{(0)} | \hat{\mathcal{L}}(\hat{F}_X - \langle \hat{F}_X \rangle) | \tilde{\varphi}^{(0)} \rangle}{\langle \tilde{\varphi}^{(0)} | \hat{\mathcal{L}} | \tilde{\varphi}^{(0)} \rangle}$$

$$\Delta_{\text{M}} = \sum_{X=A,B} \frac{\langle \tilde{\varphi}^{(0)} | \hat{\mathcal{L}}(\hat{W}_X - \langle \hat{W}_X \rangle) | \tilde{\varphi}^{(0)} \rangle}{\langle \tilde{\varphi}^{(0)} | \hat{\mathcal{L}} | \tilde{\varphi}^{(0)} \rangle}$$

where  $\langle \hat{F}_X \rangle$  and  $\langle \hat{W}_X \rangle$  are the expectation values of the operators  $\hat{F}_X$  and  $\hat{W}_X$  with  $\tilde{\varphi}_X$  for  $X = A, B$ .

It has been shown that when the Slater determinants for the isolated monomers are constructed from the exact Hartree–Fock orbitals<sup>10</sup> or when the orbitals are calculated in the dimer atomic basis set,<sup>12</sup>  $\Delta_{\text{L}} = 0$  and<sup>13</sup>  $\Delta_{\text{M}} = O(S^4)$ , where  $S = (\langle \rho_A | \rho_B \rangle)^{1/2}$  is an overlap integral of the two charge distributions,  $\rho_A$  and  $\rho_B$ .

In our study, the basis sets employed are the Dunning's d-aug-cc-pVDZ.<sup>14</sup> The Landshoff  $\Delta_{\text{L}}$  turned out to be as small as 10<sup>-8</sup> kcal/mol, which is the result of using the “dimer” basis set, while the Murrell delta has been calculated as being on the order of 0.05 kcal/mol for all of the molecules under study (as compared to 5 kcal/mol for  $E_{\text{rep}}$ ).

The geometries of all of the molecules under study have been first optimized within the atomic basis set chosen. The methane geometry corresponds to  $r_{\text{CH}} = 1.086$  Å, for the ammonia molecule  $r_{\text{NH}} = 0.998$  Å, and the HNH angle is equal to 108.11°; the water molecule geometry corresponds to  $r_{\text{OH}} = 0.941$  Å and  $\alpha_{\text{HOH}} = 104.69^\circ$ , while the hydrogen fluoride bond length is equal to 0.897 Å.

## III. Results and Discussion

Figure 1a–d shows the positions of the helium atoms at the 5 kcal/mol isosurface of the valence repulsion energy, together with the values of the Pauli hardnesses,  $h^{(1)}$  (the numbers closer to the helium atom positions), and hyperhardnesses,  $h^{(2)}$  (outer numbers), for the four molecules under study. Although the whole surfaces of the molecules have been investigated, for the sake of clarity Figure 1 shows only some sections of the surfaces.

**Shape of the Isosurface.** The valence repulsion isosurface, as well as the (first and higher) Pauli hardnesses, as functions of the position on the isosurface necessarily exhibit the

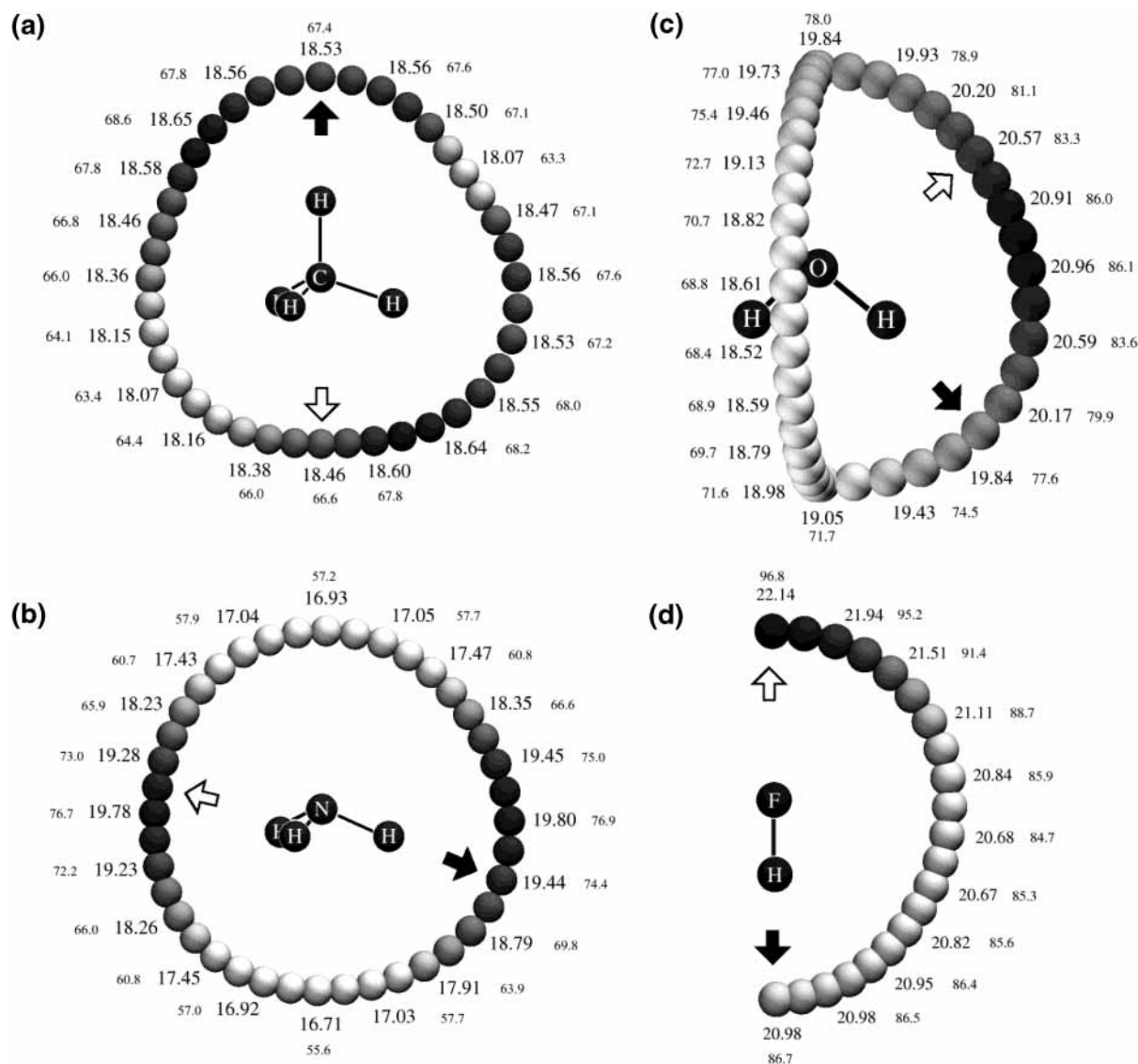


**Figure 1.** The (selected) helium atomic probe positions on the +5 kcal mol<sup>-1</sup> isosurface of the valence repulsion energy,  $E_{rep}$ : (a)  $CH_4$ ; (b)  $NH_3$ ; (c)  $H_2O$ ; (d)  $HF$ . The shadow degree of the helium probe corresponds to the value of the Pauli hardness when the probe penetrates the molecule in the direction normal to the isosurface. The numbers closest the probe positions (larger size) are the Pauli hardnesses  $h^{(1)}$  in kcal mol<sup>-1</sup> Å<sup>-1</sup>; the outer numbers (smaller size) correspond to the values of the first hyperhardness  $h^{(2)}$  in kcal mol<sup>-1</sup> Å<sup>-2</sup>. The light (black) arrow shows one of the points of the isosurface that is the closest to (most distant from) the heavy atom.

symmetry of the molecule, that is, transform according to its fully symmetric irreducible representation.

The isosurfaces turned out to be convex in all cases under study, in agreement with the previous investigations.<sup>7</sup> As seen from Table 1, the distance from the heavy atom nucleus to the isosurface depends significantly on the direction chosen. Interestingly, the amplitude,  $\Delta r = r_{max} - r_{min}$  (column 10), is very much the same (0.37 Å) for  $NH_3$ ,  $H_2O$ , and  $HF$  molecules, while the methane molecule represents an exception with  $\Delta r = 0.49$  Å.

**Pauli Hardness.** Table 1 collects the values of the maximum and minimum hardnesses ( $h_{max}^{(1)}$  and  $h_{min}^{(1)}$ , respectively), as well as the maximum and minimum X...He distances ( $r_{max}$  and  $r_{min}$ , respectively) and those X...He distances that correspond to parts of the molecules with the most Pauli hardness and most Pauli softness ( $r(h_{max}^{(1)})$  and  $r(h_{min}^{(1)})$ , respectively).

As one can see from Table 1, the valence repulsion isosurface for a given molecule differs widely by its local Pauli hardness,  $h^{(1)}$ . As seen from column 2, the Pauli maximum hardness ( $h_{max}^{(1)}$ ) for a given molecule changes monotonically in the

homological series studied: the part with the greatest Pauli hardness is in the hydrogen fluoride molecule, and the corresponding Pauli hardness amounts to 22.14 kcal mol<sup>-1</sup> Å<sup>-1</sup>, while the corresponding number for the other side of the homological series (the methane molecule) is equal to 18.66 kcal mol<sup>-1</sup> Å<sup>-1</sup>. The dependence of this quantity on the X atom atomic number is almost linear (the correlation coefficient equals to 0.9991).

The parts of the molecules with the greatest Pauli softness [or the least hard parts, that is, those corresponding to  $h_{min}^{(1)}$  defined as the minimum value of  $h^{(1)}$  on the  $E_{rep}$  isosurface] exhibit a different behavior among the members of the homological series. The minimal Pauli hardness changes in the series also almost linearly from 20.66 kcal mol<sup>-1</sup> Å<sup>-1</sup> for the hydrogen fluoride to 16.71 kcal mol<sup>-1</sup> Å<sup>-1</sup> for the ammonia molecule, but the methane molecule represents again a remarkable exception with the value  $h_{min}^{(1)} = 18.07$  kcal mol<sup>-1</sup> Å<sup>-1</sup>. This indicates that what makes the molecules soft are lone pairs, because only the methane molecule does not have one.

Because of the methane exception, the Pauli hardness anisotropy (the difference between the Pauli maximum hardness

**TABLE 1: Comparison of the First Hardnesses ( $h^{(1)}$  in kcal/(mol Å)) for the Methane, Ammonia, Water, and Hydrogen Fluoride Molecules in Their Equilibrium Hartree–Fock Geometries**

	$h_{\max}^{(1)a}$	$h_{\min}^{(1)b}$	$\Delta h^{(1)c}$	$\alpha_{\text{HeXH}}^d$	$r(h_{\max}^{(1)e})$	$r_{\max}^f$	$r(h_{\min}^{(1)g})$	$r_{\min}^h$	$\Delta r^i$
CH <sub>4</sub>	18.66	18.07	0.59	42.7	2.54	2.86	2.52	2.37	0.49
NH <sub>3</sub>	19.94	16.71	3.23	43.9	2.42	2.66	2.49	2.29	0.37
H <sub>2</sub> O	20.96	18.52	2.44	44.2	2.32	2.53	2.31	2.16	0.37
HF	22.14	20.66	1.48	180.0	2.03	2.40	2.16	2.03	0.37

<sup>a</sup> The maximum value of the first hardness. <sup>b</sup> The minimum value of the first hardness. <sup>c</sup> The difference between  $h_{\max}^{(1)}$  and  $h_{\min}^{(1)}$ . <sup>d</sup> The HeXH angles (in deg, X refers to the heavy nucleus), where the helium atom position corresponds to the maximum first hardness. <sup>e</sup> The HeX distance (Å) that corresponds to the maximum first hardness. <sup>f</sup> The maximum HeX distance (Å) on the +5 kcal/mol repulsion energy isosurface. <sup>g</sup> The HeX distance (Å) that corresponds to the minimum first hardness. <sup>h</sup> The minimum HeX distance (Å) on the +5 kcal/mol repulsion energy isosurface. <sup>i</sup>  $\Delta r = r_{\max} - r_{\min}$ .

and the Pauli minimum hardness,  $\Delta$  of Table 1) does not represent a monotonic function of the heavy atom atomic number. Due to the anomalous Pauli softness of the methane, its anisotropy also represents an exception ( $\Delta = 0.59 \text{ kcal mol}^{-1} \text{ \AA}^{-1}$ ).

Despite the fact that the molecules studied are simple, the hardness distribution over the molecular surface is quite complicated. There are usually a few maxima and a few minima for the Pauli hardness for any of the molecules. It turned out (Figure 1) that the second hardness is nearly proportional to the first one, thus suggesting an exponential increase of the valence repulsion with the probe penetration distance from the isosurface. If the dependence of the valence repulsion changed exponentially  $E_{\text{rep}} = A \exp(-Br)$ , when the atomic probe crossed the molecular boundary (isosurface of +5 kcal/mol), then the quantity  $(h^{(1)}/E_{\text{rep}} - h^{(2)}/h^{(1)})/(h^{(1)}/E_{\text{rep}})$  would have been equal to zero, whereas for the molecules under study one obtains the value as being on the order of 0.014–0.025 (i.e., about 1–2% off).

The methane (Figure 1a) has as much as 12 maxima and 10 minima of the Pauli hardness  $h^{(1)}$ . The minima positions are of two kinds: the six global minima are in the midway between any two CH directions, while the four others correspond to the CH directions. The maxima of the Pauli hardness are at the midway between any two nearest-neighbor global minima directions and are related by symmetry.

The ammonia (Figure 1b) has two Pauli hardness minima and three Pauli hardness maxima. Both minima have a similar depth (they differ by about  $0.22 \text{ kcal mol}^{-1} \text{ \AA}^{-1}$ ); the local minimum is along the lone pair direction, the global one corresponds to the opposite direction. The maxima of the Pauli hardness are located in the lone pair–NH plane roughly along the direction of the NH bonds (rotated however to a considerable extent toward the lone pair direction).

The water molecule (Figure 1c) has two symmetric Pauli hardness maxima and two symmetric minima. A maximum is within the molecular plane and corresponds to the two spots pointed roughly by the normal to the  $C_2$  axis going through the oxygen atom. A minimum of the Pauli hardness is nearly above (and below) the midpoint between the protons (taking the molecular plane as a reference level).

Figure 1d shows that the hydrogen fluoride has two maxima of the Pauli hardness on the molecular axis separated by the annular energy well extending about the molecular axis. The maximum corresponding to the fluorine atom position is larger by about  $1.16 \text{ kcal mol}^{-1} \text{ \AA}^{-1}$ .

Table 1 and Figure 1 show also that neither the  $r_{\min}$  nor the  $r_{\max}$  distances are identical to the distance of the heavy atom to the spots with the most Pauli hardness or the most Pauli softness on the isosurface. As seen from column 5 of Table 1, the maximum Pauli hardness is related to the XH direction. This time, the hydrogen fluoride represents an exception. Indeed, for

all of the molecules but hydrogen fluoride, the  $\alpha_{\text{HeXH}}$  angle varies within a quite narrow range of  $42.7^\circ$ – $44.2^\circ$ , while for the hydrogen fluoride one obtains  $\alpha_{\text{HeXH}} = 180^\circ$ . The direction of the minimum Pauli hardness in the homological series, as witnessed by the methane case, is related to the presence of lone pairs. However, only in the case of the ammonia molecule, the lone pair direction means a soft part of the molecule (although even in this case the opposite direction is a little softer). In the hydrogen fluoride and water cases, the minimum Pauli hardness direction is always between the lone pair and the XH direction.

For the systems under study, there are available high-accuracy computations for their complexes with rare gas atoms. The computations take into account the SAPT high-level intramonomer electronic correlation effects. For the methane molecule, only the data for its complex with the argon atom are available. It turns out that each of the global minima found in such calculations<sup>15</sup> corresponds to our cluster of the three global maxima (faces of the tetrahedron) of the Pauli hardness  $h^{(1)}$ . For the ammonia molecule, no data are available. For the water molecule with the helium atom complex, the global minimum direction given as the CM–O–He angle (CM is the center of mass) has been computed as being equal to  $90^\circ$ ,  $80^\circ$ ,  $75^\circ$ ,  $78.3^\circ$ , and  $75^\circ$  in refs 16–20, respectively. In the present paper, the angle corresponding to the spot with the greatest Pauli hardness of the water molecule is quite close to those values and amounts to  $82.3^\circ$ . In the case of the hydrogen fluoride complex with the helium atom, two electronic energy minima have been found lying on both sides of the molecular axis.<sup>21</sup> In this case, these are precisely the hardest spots of the valence repulsion energy. This time, the side with the greatest Pauli hardness side (fluorine atom) corresponds not to the global but to the local minimum of the electronic energy (the difference of the well depths is however on the order of 10% of the interaction energy). Thus, it appears that there is a rule of thumb, that the minima of the interaction potential correspond to hardest parts of the molecular surface.

#### IV. Conclusions

One may conclude the following: (1) A valence repulsion energy isosurface may be used to define the molecular shape. At any point of the isosurface, one may calculate hardness (first derivative) and hyperhardnesses (higher derivatives) as a response to the probe penetration normally to the isosurface. (2) The Pauli hardnesses differ widely within a single molecule, thus exhibiting a strong anisotropy. (3) The distribution of the parts with the greatest Pauli hardness and Pauli softness of the molecular surface is fairly complicated. The maximum Pauli hardness directions are related to the XH directions (although they are not identical to it), while the minimum Pauli hardness in a molecule is connected to the presence of the lone pairs

(but in general directed off the lone pair direction). (4) The maximum Pauli hardnesses, as well as the minimum Pauli hardnesses, differ widely in the homological series that we have investigated showing a monotonic dependence on the heavy atom atomic number (with a remarkable exception of the methane molecule minimum hardness), (5) Interestingly, the hardest parts of the valence repulsion isosurface often correspond to the global minimum of the interaction energy. (6) The Pauli second hardness is to a good accuracy proportional to the first one.

**Acknowledgment.** This work was supported by the KBN PhD grant. All calculations have been carried out using the SAPT program written in cooperation between the University of Warsaw and the University of Delaware research groups.

### References and Notes

- (1) Hirschfelder, J. O.; Curtiss, C. F.; Bird, R. B. *Molecular Theory of Gases and Liquids*; Wiley: New York, 1964.
- (2) Buckingham, A. D.; Fowler, P. W.; Hutson, J. M. *Chem. Rev.* **1988**, *88*, 963.
- (3) Jeziorski, B.; van Hemert, M. *Mol. Phys.* **1976**, *31*, 713.
- (4) Dykstra, C. E. *Chem. Rev.* **1993**, *93*, 2339.
- (5) Price, S. L.; Stone, A. J. *Mol. Phys.* **1980**, *40*, 805.
- (6) Kołos, W.; Jeziorski, B. *Int. J. Quantum Chem.* **1977**, *12* (Suppl. 1), 91.
- (7) Amovilli, C.; McWeeny, R. *J. Mol. Struct. (THEOCHEM)* **1991**, *227*, 1.
- (8) Stone, A. J.; Tong, C. S. *J. Comput. Chem.* **1994**, *15*, 1377.
- (9) Gilbert, T. L.; Simpson, O. C.; Williamson, M. A. *J. Chem. Phys.* **1975**, *63*, 4061.
- (10) Landshoff, R. *Z. Phys.* **1936**, *102*, 201.
- (11) Murrell, J. N.; Varandas, A. J. C. *Mol. Phys.* **1975**, *30*, 223.
- (12) Gutowski, M.; Chałasiński, G.; van Duijneveldt-van de Rijdt, J. *Int. J. Quantum Chem.* **1984**, *26*, 971.
- (13) Jeziorski, B.; Bulski, M.; Piela, L. *Int. J. Quantum Chem.* **1976**, *10*, 281.
- (14) Dunning, T. H., Jr. *J. Chem. Phys.* **1989**, *90*, 1007. Woon, D. E.; Dunning, T. H., Jr. *J. Chem. Phys.* **1994**, *100*, 2975.
- (15) Heijmen, T. G. A.; Korona, T.; Moszyński, R.; Wormer, P. E. S.; van der Avoird, A. *J. Chem. Phys.* **1997**, *107*, 902.
- (16) Patkowski, K.; Korona, T.; Moszyński, R.; Jeziorski, B.; Szalewicz, K. *J. Mol. Struct. (THEOCHEM)* **2002**, *591*, 231.
- (17) Maluendes, S.; McLean, A. D.; Green, S. *J. Chem. Phys.* **1992**, *96*, 8150.
- (18) Kukawska-Tarnawska, B.; Chałasiński, G.; Szczeniński, M. M. *J. Mol. Struct. (THEOCHEM)* **1993**, *297*, 313.
- (19) Tao, F. M.; Li, Z.; Pan, Y. K. *Chem. Phys. Lett.* **1996**, *255*, 179.
- (20) Hodges, M. P.; Wheatley, R. J.; Harvey, A. H. *J. Chem. Phys.* **2002**, *116*, 1397.
- (21) Moszyński, R.; Wormer, P. E. S.; Jeziorski, B.; van der Avoird, A. *J. Chem. Phys.* **1994**, *101*, 2811.